Published online 10 July 2018

Nucleic Acids Research, 2018, Vol. 46, No. 14 ***7379–7395***
doi: 10.1093/nar/gky615

SRSF9 selectively represses ADAR2-mediated editing of brain-specific sites in primates

Raghuvaran Shanmugam[1,2,†], Fan Zhang[2,†], Harini Srinivasan[1,2], John Lalith Charles Richard[2], Kaiwen I. Liu[2], Xiujun Zhang[1,2], Cheok Wei A. Woo[2], Zi Hao M. Chua[2,3], Jan Paul Buschdorf[4], Michael J. Meaney[4,5] and Meng How Tan[1,2,*]

[1]School of Chemical and Biomedical Engineering, Nanyang Technological University, Singapore 637459, Singapore, [2]Genome Institute of Singapore, Agency for Science Technology and Research, Singapore 138672, Singapore, [3]School of Life Sciences and Chemical Technology, Ngee Ann Polytechnic, Singapore 599489, Singapore, [4]Singapore Institute for Clinical Sciences, Agency for Science Technology and Research, Singapore 117609, Singapore and [5]Douglas Mental Health University Institute, McGill University, Montreal (Quebec) H4H 1R3, Canada

Received October 24, 2017; Revised June 21, 2018; Editorial Decision June 25, 2018; Accepted June 26, 2018

ABSTRACT

Adenosine-to-inosine (A-to-I) RNA editing displays diverse spatial patterns across different tissues. However, the human genome encodes only two catalytically active editing enzymes (ADAR1 and ADAR2), suggesting that other regulatory factors help shape the editing landscape. Here, we show that the splicing factor SRSF9 selectively controls the editing of many brain-specific sites in primates. SRSF9 is more lowly expressed in the brain than in non-brain tissues. Gene perturbation experiments and minigene analysis of candidate sites demonstrated that SRSF9 could robustly repress A-to-I editing by ADAR2. We found that SRSF9 biochemically interacted with ADAR2 in the nucleus via its RRM2 domain. This interaction required the presence of the RNA substrate and disrupted the formation of ADAR2 dimers. Transcriptome-wide location analysis and RNA sequencing revealed 1328 editing sites that are controlled directly by SRSF9. This regulon is significantly enriched for brain-specific sites. We further uncovered a novel motif in the ADAR2-dependent SRSF9 binding sites and provided evidence that the splicing factor prevents loss of cell viability by inhibiting ADAR2-mediated editing of genes involved in proteostasis, energy metabolism, the cell cycle and DNA repair. Collectively, our results highlight the importance of SRSF9 as an editing regulator and suggest potential roles for other splicing factors.

INTRODUCTION

Adenosine-to-inosine (A-to-I) RNA editing is a prevalent post-transcriptional gene regulatory mechanism (1). Recent high-throughput sequencing studies of the transcriptome of multiple organisms from *Caenorhabditis elegans* and *Drosophila* to mice and humans have uncovered a large number of editing sites, the vast majority of which are of the A-to-I type (2–11). In humans, there are over a million A-to-I editing sites, especially in *Alu* repetitive regions due to the formation of long and stable double-stranded RNA (dsRNA) structures. Since inosines are recognized by cellular machineries as guanosines, the editing events are effectively nucleotide substitutions that alter the sequences of the final RNA transcripts. Consequently, RNA editing can result in new protein isoforms, affect RNA splicing, influence RNA stability, alter microRNA targets and impact on the maturation of microRNAs among others. Aberrant editing in humans is known to contribute to various diseases, including multiple cancer types (12–14) and various neurological disorders (15–18). Given the far-ranging impact of RNA editing, it must be carefully orchestrated to ensure normal cell physiology and organismal health.

The ADAR family of enzymes catalyzes the deamination reaction in A-to-I RNA editing (1). There are three ADAR genes (ADAR1, ADAR2 and ADAR3) annotated in the mammalian genome. Besides a deaminase domain located at the C-terminus, each ADAR protein contains two to three dsRNA-binding domains. However, ADAR3 has no known editing activity and its function in the brain, where it is solely expressed, remains unresolved. On the other hand, ADAR1 and ADAR2 are expressed in multiple tissues (19) and have clear demonstrable editing activities that are essential for many biological processes. Both the ADAR1 knockout mouse (20–22) and the ADAR1

*To whom correspondence should be addressed. Tel: +65 6513 8063; Fax: +65 6794 7553; Email: mh.tan@ntu.edu.sg
†The authors wish it to be known that, in their opinion, the first two authors should be regarded as Joint First Authors.

editing-deficient mouse (23) are embryonic lethal, while the ADAR2 knockout mouse dies within 20 days of birth from epileptic seizures (24). These animal models again underscore the necessity for RNA editing to be under tight spatiotemporal control.

Due to their critical importance in normal physiology and diseases, the editing activities of the ADAR enzymes are highly regulated at the transcriptional, post-transcriptional and post-translational levels. The expression of the ADAR1 p150 isoform is induced by interferons (25,26), while the expression of ADAR2 is stimulated by the CREB transcription factor (27) but downregulated by thiamine deficiency (28). At the post-transcriptional level, alternative splicing results in multiple ADAR isoforms with different editing efficiencies (29). Furthermore, the ADAR2 pre-mRNA is known to undergo editing itself, which subsequently influences the splicing process. Post-translationally, sumoylation of ADAR1 by SUMO1 lowers the activity of the enzyme (30), while ubiquitination of ADAR2 by the E3 ubiquitin ligase WWP2 enhances the degradation of the protein (31). We have also recently found that degradation of both the ADAR1 and ADAR2 enzymes is regulated by an aminoacyl tRNA synthetase complex-interacting protein AIMP2 (19). In addition, various studies have demonstrated that subcellular localization of the ADAR enzymes is another important mechanism to regulate RNA editing activity (31–33).

Recently, we have performed an extensive profiling of A-to-I RNA editing in thousands of human samples from the Genotype-Tissue Expression (GTEx) project and in hundreds of additional primate and mouse samples (19). Our study revealed a highly dynamic landscape of editing, including diverse spatial patterns of editing across tissues. Since there are only two catalytically active adenosine deaminases, we hypothesize that there must be many other non-ADAR regulators that help shape the editing landscape. One intriguing observation that we made was that in all the mammalian species that we examined, many protein-coding sites were more highly edited in brain than in non-brain tissues. In the mouse, this finding is unsurprising because editing levels are highly correlated with ADAR1 and/or ADAR2 expression levels both across tissues and over development (19). However, we did not observe this correlation in human, thereby prompting us to search for an alternative factor that may help explain why particular sites are more highly edited in the human brain than in non-brain tissues, despite a more ubiquitous expression of ADAR1 and ADAR2.

Here, we report that the splicing factor SRSF9 is a key factor that serves to restrict the editing of numerous protein-coding and non-coding sites to the brain. SRSF9, also known as SRp30c, belongs to an evolutionarily conserved serine/arginine-rich (SR) family of splicing factors, which performs fundamental roles both in constitutive and also in alternative pre-mRNA splicing (34). SRSF9, in particular, has been found to regulate the alternative splicing of multiple disease-associated genes, like hnRNP A1 (35), tau (36) and Bcl-x (37). In addition, besides splicing, SR family members are known to participate in various mRNA metabolic processes, including nuclear export, nonsense-mediated decay and translation (38,39). More recently, SRSF9 was found to repress ADAR2-mediated editing through a genetic screen (40). Motivated by this work, we found that the expression of SRSF9 was generally lower in the brain than in non-brain tissues. Subsequently, we demonstrated, through a combination of genetics, biochemical and genomics approaches, that SRSF9 repressed editing by potentially interfering with the dimerization of ADAR2 in the nucleus and also delineated the direct editing regulon of SRSF9, which was significantly enriched for brain-specific sites. We further uncovered a novel sequence motif in the ADAR2-dependent SRSF9 binding sites that may help account for some of the brain-specific editing observed in humans. Collectively, our results underscored the importance of splicing factors in sculpting the editing landscape in humans and also potentially other non-human primates.

MATERIALS AND METHODS

Plasmids

We cloned human ADAR2 into either pcDNA4A or p3xFLAG-CMV10. We also utilized a published expression construct for ADAR2 (41). Additionally, we cloned SRSF9 into pcDNA4A or pEF6-V5-His with a STOP codon introduced between the C-terminal V5 and His tags by site-directed mutagenesis. Mutations in SRSF9 were created using QuikChange Lightning Site-Directed Mutagenesis Kit (Agilent) following manufacturer's instructions. All minigenes were cloned into pcDNA3.

Cell lines, viral production and transfection

HEK293T cells were grown in Dulbecco's modified Eagle's medium (DMEM) supplemented with 10% fetal bovine serum (FBS) (Hyclone) and Penicillin-Streptomycin (Gibco). The cells were split into a 6-well plate the day before transfection, so that they would be around 80% confluent the next day. Cells were transfected using JetPrime transfection reagent following manufacturer's instructions. A total of 0.75 μg ADAR2 expression vector and 1.5 μg SRSF9 expression vector were used for transfection.

SH-SY5Y cells were grown in DMEM-F12 supplemented with 10% FBS (Hyclone). We used lentiviral transduction to overexpress ADAR2 in SH-SY5Y. Standard protocol was followed to generate viruses. Briefly, pCSII-EF-ADAR2-IRES-Venus was packed using VsVg and PAX2 lentiviral package system in HEK293FT cells. The supernatant containing viral particles were collected at 24 and 48 h after transfection and concentrated using centrifugal cut-off filters (Millipore). The concentrated viral particles were used to infect SH-SY5Y cells grown in 6-well plates. The cells were sorted by flow cytometry 3–4 days after transduction.

RNA isolation and qRT-PCR

Total RNA was extracted from cells using the TRIzol reagent (Invitrogen) and was then purified using Zymo RNAmini columns with on-column DNase I digestion (Zymo research). The concentration of RNA was determined by NanoDrop 2000 (ThermoScientific). A total of

1 μg DNase-treated total RNA was reverse transcribed with oligo(dT) and SuperScript III (Invitrogen). Quantitative real-time polymerase chain reaction (qRT-PCR) was performed with 1 μl 5-fold diluted cDNA and 2X KAPA SYBR Green (KapaBiosystems) in a 10 μl reaction on a PRISM 7900HT system (Applied Biosystems).

RNA editing analysis

Each region-of-interest was amplified from cDNA samples using REDiant 2× Taq Mastermix (first Base), purified, and then sent for Sanger sequencing (Axil Scientific). Editing was quantified by dividing the height of G peak with the sum of A and G peak heights. All measurements were made in Adobe Photoshop CS5.

Cell lysis and western blot

Cells were lysed in RIPA buffer containing protease inhibitor cocktail (Roche) and 1 mM phenylmethylsulfonyl fluoride (PMSF). Equal amount of protein lysate was resolved on a 10% sodium dodecyl sulfate-polyacrylamide gel electrophoresis (SDS-PAGE) and transferred to a nitrocellulose membrane (Millipore) using fast Turbo Transfer (Bio-rad). After blocking in 5% skimmed milk for 1 h, the appropriate primary antibody was added: anti-ADAR2 (RED1) (1:1000, ab64830, Abcam), anti-SRp30c(SRSF9) (1:1000, sc-134036, Santa Cruz), anti-FLAG (1:2000, Clone M2, Sigma), anti-cMyc (1:1000, sc-789, Santa Cruz), anti-V5 (1:2000, ab9116, Abcam) or anti-β-actin (1:1000, clone C4, sc-47778, Santa Cruz). Primary antibodies were incubated overnight in the cold room. After washing with phosphate-buffered saline (PBS)/0.2% Tween-20 (PBST), a secondary antibody, namely horse-radish peroxidase (HRP)-conjugated anti-rabbit IgG (1:5000, NA934V, Amersham) or HRP-conjugated anti-mouse IgG (1:5000, NA931V, Amersham), was added for 1 h. After washing with PBST, signals were detected using the WesternBright Sirius Chemiluminescent HRP Substrate (Advansta).

Co-immunoprecipitation and native PAGE analysis

HEK293T cells (2×10^6) were transfected with the relevant tagged constructs, which included FLAG-tagged ADAR2, MYC-tagged SRSF9 and V5-tagged SRSF9. Forty-eight hours after transfection, the cells were lysed in RIPA buffer containing 50 mM Tris–HCl (pH 7.45), 150 mM NaCl, 0.1% SDS, 1 mM EDTA, 10 mM sodium fluorite, 0.5% Nonidet P-40, 0.1 mM phenylmethylsulfonyl fluoride (pH 7.5) and a protease inhibitor cocktail (Roche). Cleared cell lysates were incubated with anti-FLAG M2 affinity beads (Sigma) overnight at 4°C followed by 2× RIPA washes and eluted in gel loading buffer (150 mM Tris–HCl (pH 7.0), 12% SDS, 25% glycerol, 0.05% bromophenol blue and 6% β-mercaptoethanol). The samples were separated by 10% SDS-PAGE, transferred onto a nitrocellulose membrane, and probed with specific antibodies, which included anti-FLAG, anti-MYC or anti-V5. To study ADAR2 dimer disruption by SRSF9, the samples were eluted in loading buffer without β-mercaptoethanol and resolved by native PAGE without SDS.

RNA-seq library construction

Poly(A) mRNAs were first obtained from 2 μg total RNA using NEBNext Poly(A) mRNA Magnetic Isolation Module (New England Biolabs). The resultant mRNAs were then processed using the NEBNext Ultra Directional RNA Library Prep Kit (New England Biolabs) according to manufacturer's instructions. Pooled barcoded samples were then sequenced on the Illumina HiSeq platform.

Enhanced CLIP

Enhanced CLIP (eCLIP) experiments were performed according to a published protocol with modifications (42). Briefly, HEK293T cells overexpressing SRSF9 (with or without ADAR2 overexpression) were ultraviolet-irradiated at 254 nm (UV-C), 1500 mJ cm^2 (Stratagene Stratalinker). Subsequently, the cells were lysed in iCLIP lysis buffer with short pulses of sonication using the bioruptor. DNA was removed from the cell lysate by Turbo DNase treatment and RNA was fragmented by 5 min-treatment with RNase I at 37°C. The cleared lysates were incubated with MYC-coupled Protein G Dynabeads (Invitrogen) for 4 h at 4°C, and then eluted and transferred overnight onto nitrocellulose membrane. RNA–protein complex were cut and the bound complex was treated with Proteinase K (New England Biolabs) to remove the proteins. The RNA was then extracted by phenol:chloroform method and concentrated using RNA Clean & Concentrator-5 (Zymo research). The eluted RNA was reverse transcribed, ligated with adaptors and PCR amplified to make the library.

Cell viability and apoptosis assays

Cell viability was measured using PrestoBlue (Thermofisher) following manufacturer's protocol. Briefly, 20 000 cells were seeded in triplicates in a 96-well plate for each condition. After 24 h of incubation in normal growth medium, the cells were washed with PBS and 1:10 PrestoBlue in DMEM-F12 was added to the cells, which were then left in a CO_2 incubator at 37°C for 30 min. Fluorescence measurements were taken using SpectraMax Plus 384 Microplate Reader. For the apoptosis assay, 20 000 cells were seeded in a 24-well plate and grown in a CO_2 incubator for 24 h. The cells were then treated with 1 μM staurosporine for 1 h before they were harvested by trypsinization for Alexa Fluor 647 annexin V staining (Thermofisher). All microscopy images were taken using EVOS FLoid Cell Imaging Station.

Illumina sequencing data analysis

To process the data, we first mapped the reads against the human genome assembly hg19 with STAR (mismatch penalty parameter was –outFilterMismatchNmax 15). Uniquely mapped reads with mapping quality ≥20 were reordered, sorted and assigned group information. Duplicates were removed using Picard. Local realignment and recalibration were then performed with GATK toolkit. Variants were next called by samtools mpileup against the position list from RADAR editing database (human hg19

all sites) and filtered with minimum coverage threshold (20 reads per site).

To determine whether there was any enrichment for brain-specific editing sites in the SRSF9 regulon, we tried three different backgrounds. The first background was all the editing sites within the 683 significant genes whose editing was not affected by SRSF9 overexpression based on our RNA-seq data. The second background was all sites that were covered by at least 20 sequencing reads in our RNA-seq data but were not regulated by SRSF9. The third background was all non-significant sites with a minimum coverage of 20 reads in our RNA-seq data and a minimum editing frequency of at least 5% in at least one GTEx tissue.

RESULTS

Brain-specific RNA editing of protein-coding sites in mammals

In our recent effort to construct a comprehensive RNA editing atlas in mammals (19), we observed that many protein-coding sites were more highly edited in the brain than in non-brain tissues. We applied microfluidic multiplexed PCR (mmPCR-seq) (43) on multiple tissues from a single human individual (N37) and observed that although the overall editing profiles across the different tissues appeared to be generally similar partly due to the presence of primate-specific Alu repeats, many editing sites in protein-coding regions of the transcriptome appeared to be brain-specific, including well-known recoding sites in receptors or ion channels involved in neurotransmission, such as HTR2C (44), GRIK2 (45), GABRA3 (46) and KCNA1 (47) (Figure 1A). Transcriptome analysis of the same tissues by RNA sequencing (RNA-seq) revealed that although some of the sites were located in genes that were specifically or more highly expressed in the brain, the majority of these sites were present in genes that were well expressed in non-brain tissues (Figure 1B).

Since the brain-specific protein-coding sites were identified from a single human individual, we examined the editing levels of these sites in the GTEx tissue samples. Similar to our mmPCR-seq results, we again observed that the sites were more highly edited in the brain than in non-brain tissues ($P < 1 \times 10^{-16}$, Student's *t*-test) (Supplementary Figure S1). Notably, while some of the sites were located in genes that were exclusively or more highly expressed in the brain (Supplementary Figure S2), most of them were present in genes that were widely expressed throughout the human body (Supplementary Figure S3). Hence, expression of the host genes could not adequately account for the brain-specific editing of these protein-coding sites.

We sought to determine what *trans*-acting factor(s) may contribute to brain-specific editing of selected sites. In the mouse, both ADAR1 and ADAR2 are more highly expressed in brain regions than in non-brain tissues (19). However, when we examined the transcript levels of ADARs in human, we did not observe a similar trend. In the N37 human individual, both ADAR1 and ADAR2 were more highly expressed in the lung than in the cerebellum or frontal lobe (Figure 1C). Although we found that the expression of ADAR3 was highly brain-specific, this particular deaminase possessed no known catalytic activity and we had also previously provided evidence that it may function as an inhibitor of editing instead (19). Likewise, in the GTEx samples, ADAR1 and ADAR2 were broadly expressed throughout the human body, while ADAR3 was highly enriched in the brain regions (Supplementary Figure S4).

Next, we examined the expression levels of non-ADAR regulators of editing. Strikingly, we observed that the transcript levels of the splicing factor SRSF9 appeared to be generally low in brain regions and higher in non-brain tissues for both the N37 individual (Figure 1C) and the GTEx samples (Supplementary Figure S4). Since SRSF9 was previously shown to repress the editing of two substrates, CYFIP2 and CFLAR (40), it served as a potential candidate factor for us to subsequently follow-up. Notably, CYFIP2 was also a gene whose editing we had found to be highly brain-specific (Figure 1A and Supplementary Figure S1).

To corroborate our observations in human, we checked the expression levels of the ADAR enzymes and SRSF9 as well as the editing levels of several protein-coding sites in multiple cynomolgus monkey (*Macaca fascicularis*) tissues. qRT-PCR assays showed that there was no enrichment of ADAR1 and ADAR2 transcripts in the brain, although SRSF9 was indeed more lowly expressed in the brain than in non-brain tissues (except muscles) (Figure 1D). We further confirmed the levels of SRSF9 by Western blot (Supplementary Figure S5A). Additionally, Sanger sequencing of protein-coding sites in the TMEM63B gene (Figure 1E) as well as the CYFIP2, SON and XKR6 genes (Supplementary Figure S5B–D) revealed brain-specific editing of these sites. Importantly, we found that SRSF9 expression was able to account for over 75% of the editing of brain-specific sites in both human and *M. fascicularis* (Supplementary Figure S6). Collectively, our results suggested that SRSF9, but not ADAR1 or ADAR2, may enable brain-specific editing of selected sites in humans and non-human primates.

Editing repression of endogenous substrates by SRSF9

We first performed gene perturbation experiments in HEK293T cells to assess our hypothesis that SRSF9 functions as a key enabler of brain-specific editing in primates. For each target site, we transfected SRSF9 alone, ADAR1 or ADAR2 alone, or an editing enzyme together with SRSF9 (Figure 2A). We used Sanger sequencing to quantify the editing levels of 16 brain-specific protein-coding sites in ten different genes as well as three other protein-coding sites in two genes that did not exhibit brain-specific editing in the N37 human individual (Supplementary Figure S7A) and in the GTEx samples (Supplementary Figure S7B). Almost all of the editing sites tested were either not edited or were edited at low levels in the control cells and in cells transfected with only SRSF9 (Supplementary Figures S8–10). We also observed that with the exception of NEIL1, most of the genes were mainly ADAR2 targets (Figure 2B), which is consistent with our recent finding that ADAR2 is the primary editor of non-repetitive coding sites (19). Importantly, we found that SRSF9 was able to significantly repress ADAR2-mediated editing of 12 out of the 16 brain-specific sites by at least 5% ($P < 0.05$, Student's *t*-test). Only the editing of NEIL1 and NOVA1 was not repressed by the

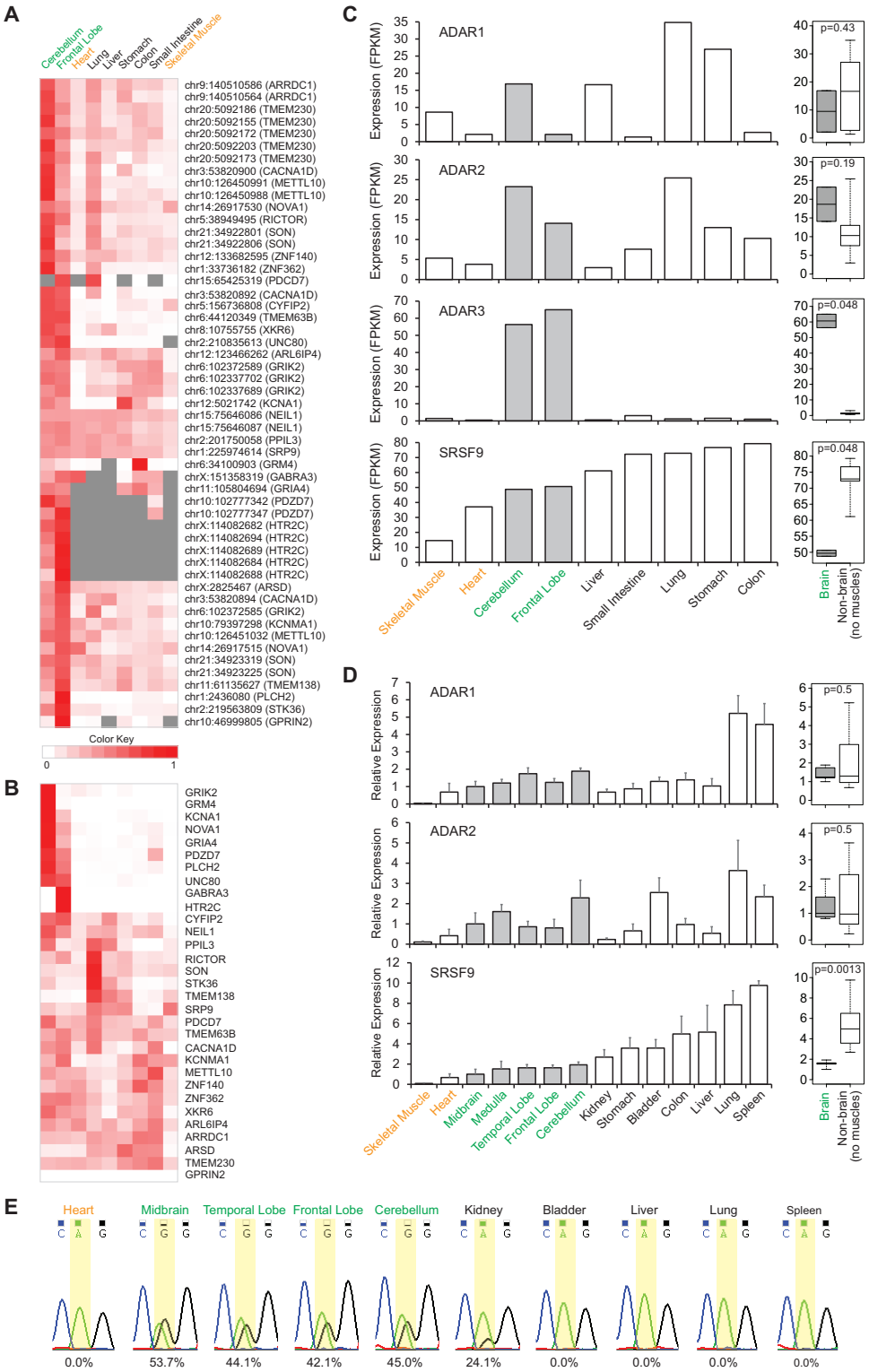

Figure 1. Editing of protein-coding sites in brain and non-brain primate tissues. (**A**) Heatmap showing the editing levels of brain-specific protein-coding sites across multiple tissues from a single human individual (N37), as determined by mmPCR-seq. (**B**) Heatmap showing the spatial expression levels of the genes whose editing exhibited brain specificity. The columns are arranged in the same order as (A). (**C**) Left: expression of the ADAR enzymes and SRSF9 across different tissues from N37, as determined by RNA-seq. The samples are sorted by the relative transcript levels of SRSF9. Right: boxplots comparing expression levels in brain tissues versus non-brain tissues (excluding skeletal muscle and heart, which can be interpreted as cardiac muscle). (**D**) Left: expression of ADAR1, ADAR2 and SRSF9 in multiple Cynomolgus monkey tissues, as determined by qRT-PCR. The samples are sorted by the relative transcript levels of SRSF9. Error bars indicate the s.e.m. ($n = 3$ biological replicates). Right: Boxplots comparing expression levels in brain tissues versus non-brain tissues (excluding skeletal muscle and heart). (**E**) Exemplary chromatograms showing the editing of TMEM63B in different monkey tissues.

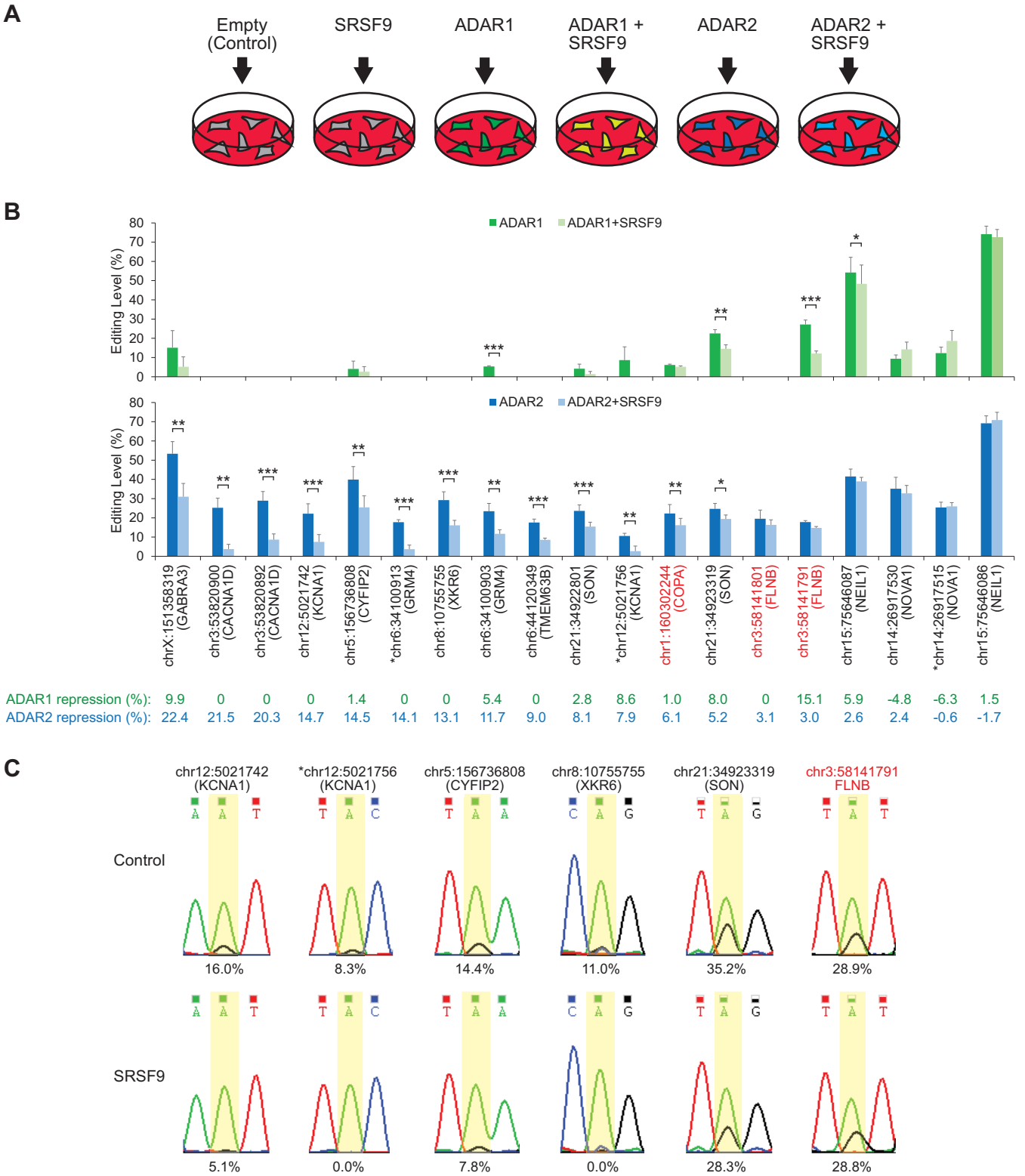

Figure 2. Repressing the editing of endogenous sites by SRSF9. (**A**) Schematic of our experimental setup to evaluate whether SRSF9 could repress ADAR1-mediated editing and ADAR2-mediated editing. (**B**) Effect of SRSF9 on A-to-I editing of endogenous sites in HEK293T cells. Hg19 coordinates are shown. Genes highlighted in red are not brain-specific. For SON, chr21:34922806 and chr21:34923225 were not edited in HEK293T cells (even with ADAR2 overexpression). Hence, we focused mainly on chr21:34922801 and chr21:34923319. Additionally, we discovered novel editing sites (indicated by asterisks next to their coordinates) in GRM4, KCNA1 and NOVA1. Error bars indicate the s.e.m. ($n \geq 3$ biological replicates). (*$P < 0.1$, **$P < 0.05$, ***$P < 0.01$; Student's t-test. All significant sites must show at least 5% change in their editing levels). (**C**) Chromatograms showing SRSF9 inhibiting the editing of protein-coding sites in a human neural progenitor cell line ReN-VM. The editing sites, chr21:34922801 (SON), chr6:44120349 (TMEM63B) and chr3:58141801 (FLNB) were not edited in ReN-VM.

splicing factor. Notably, the repression in editing of the 12 brain-specific sites was not simply due to a decrease in the expression of ADAR2 (Supplementary Figure S11A). We further observed that the editing of the non-brain-specific sites in the COPA and FLNB genes were repressed by a much smaller extent than most of the brain-specific sites.

Next, we performed gene perturbation experiments in the human neural progenitor cell line ReN-VM, which naturally expressed ADAR2 at a much higher level than HEK293T cells (Supplementary Figure S11B). Consequently, we observed that a number of protein-coding sites in the endogenous KCNA1, CYFIP2, XKR6, SON and FLNB genes were moderately edited without the need to transduce an additional plasmid to overexpress the editing enzyme (Figure 2C). Importantly, we found that overexpression of SRSF9 in the ReN-VM cells led to a reduction in the editing levels of the brain-specific sites located within KCNA1, CYFIP2, XKR6 and SON by at least 5%. In contrast, SRSF9 overexpression did not change the editing of FLNB appreciably. Collectively, our data demonstrated that SRSF9 was able to selectively repress the editing of particular protein-coding sites in human cells.

Interaction between SRSF9 and ADAR2

To gain mechanistic insights into the negative regulation of editing by SRSF9, we examined the interaction between the splicing factor and ADAR2. We first checked whether full-length FLAG-tagged ADAR2 protein and different truncated variants of the editing enzyme could biochemically interact with V5-tagged SRSF9 (Figure 3A). Consistent with a previous study (40), full-length ADAR2 was able to pull down SRSF9 in co-immunoprecipitation experiments using beads coupled with an α-FLAG antibody, while a beads-only control without any ADAR2 protein was unable to do so. We also found that the dsRBD2 and deaminase domains of ADAR2 were dispensable for the interaction between the editing enzyme and the splicing factor. Interestingly, deletion of the N-terminus (amino acids 1–77) of ADAR2 abolished the ability of the editing enzyme to pull down SRSF9, suggesting that some element within this N-terminal region was required for the interaction. We further confirmed our pull-down results with MYC-tagged SRSF9 (Supplementary Figure S12). Previous work has shown that the N-terminal region of ADAR2 contains a nuclear localization signal (NLS) (48). Hence, to determine if a NLS is the missing element, we fused an artificial SV40 NLS to construct A5 and found that we could again co-immunoprecipitate SRSF9 (Figure 3A). Collectively, our data indicate that the dsRBD1 domain of ADAR2 interacts with SRSF9 in the nucleus and are also consistent with a previous study that demonstrated a co-localization of SRSF9 and ADAR2 in the nucleoli (40).

Next, we asked which regions of SRSF9 may be important for the splicing factor to interact with the editing enzyme. Here, we evaluated whether full-length FLAG-tagged ADAR2 could pull-down different deletion fragments of V5-tagged SRSF9 in co-immunoprecipitation assays (Figure 3B). Removal of the C-terminal serine/arginine (SR)-rich domain did not impact on the ability of the splicing factor to associate with ADAR2 in a complex. However, we found that removal of either RNA recognition domain alone (RRM1 or RRM2) abolished the interaction between SRSF9 and ADAR2. Strikingly, when we fused a SV40 NLS to the RRM2 domain of SRSF9 (construct S5), interaction between the splicing factor and ADAR2 was re-established. Hence, our data indicate that the N-terminal RRM1 domain of SRSF9 may contain a cryptic NLS and that the RRM2 domain alone is sufficient to interact with the editing enzyme.

To assess the functionality of the various SRSF9 deletion fragments, we tested whether each construct could repress ADAR2-mediated editing of endogenous XKR6 transcripts in HEK293T cells (Figure 3C). Overall, truncated variants that did not co-immunoprecipitate with ADAR2 also failed to repress the editing of XKR6. Importantly, we found that construct S5 (NLS-RRM2) was able to inhibit editing to the same extent as full-length SRSF9.

In view of the fact that SRSF9, ADAR2 and the underlying RNA substrate have a tripartite relationship, we asked whether the interaction between the two proteins required the presence of the RNA. From co-immunoprecipitation experiments, we found that the interaction between SRSF9 and ADAR2 was greatly diminished upon RNase treatment (Figure 3D). A previous study also showed that a highly conserved SWQDLKD motif in RRM2 is important for the family of SR proteins to bind to RNA (49). Hence, we tested whether K128A and D129A mutations could separately impact the ability of SRSF9 to interact with ADAR2. From co-immunoprecipitation experiments, we observed that both mutations led to an obvious reduction in the amount of SRSF9 protein that was pulled down together with ADAR2 (Figure 3E). Furthermore, both SRSF9 mutants were no longer able to repress ADAR2-mediated editing of endogenous XKR6 transcripts (Figure 3F). Collectively, our data highlighted the importance of the RNA substrate in mediating the interaction between ADAR2 and SRSF9.

Since the N-terminus and dsRBD1 domain of ADAR2 had previously been shown to be necessary for protein dimerization and editing activity (50,51), we wondered whether the interaction of SRSF9 with this region of the editing enzyme (Figure 3A) would interfere with the formation of ADAR2 dimers. To test this, we immunoprecipitated ADAR2 without and with overexpression of V5-tagged SRSF9 and then resolved the protein mixture by non-denaturing native PAGE before probing for the editing enzyme and the splicing factor by Western blot (Figure 3G and Supplementary Figure S13). Strikingly, we found that overexpression of SRSF9 led to a significant decrease in the amount of ADAR2 dimers and a concomitant increase in the amount of ADAR2 monomers ($P < 0.01$, Student's *t*-test) (Figure 3H). Taken together, our results show that SRSF9 represses A-to-I editing by possibly preventing or disrupting the formation of ADAR2 dimers within the cell nucleus in a RNA-dependent manner.

Analysis of minigenes competent for ADAR2 editing and SRSF9 repression

Given the importance of the RNA substrate in mediating the interaction between SRSF9 and ADAR2, we sought

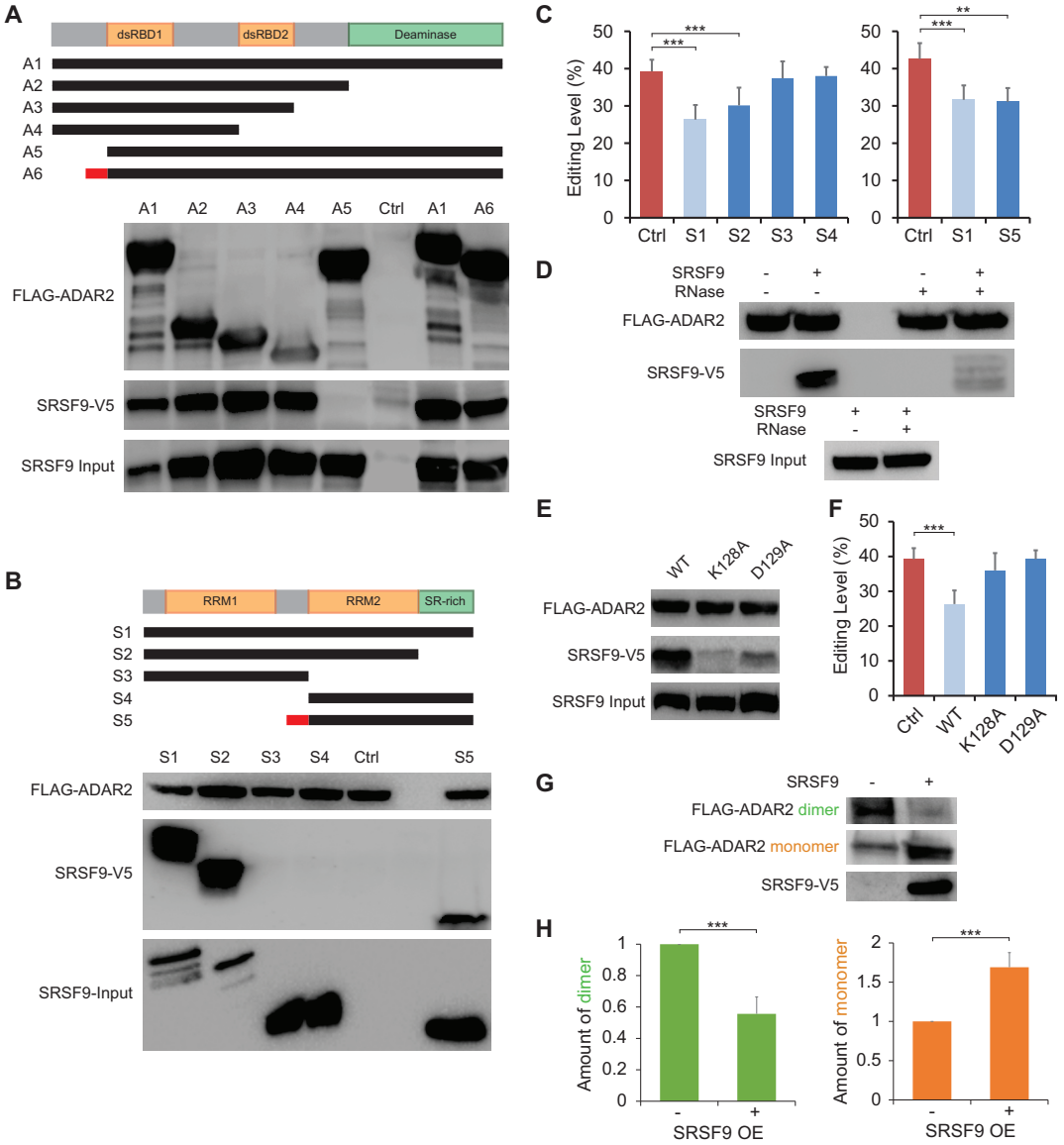

Figure 3. Interaction of SRSF9 with ADAR2. (**A**) Minimal fragment of ADAR2 that could interact with full-length SRSF9 by co-immunoprecipitation. Six different ADAR2 truncation variants (A1–A6) were tested. The short red bar in the schematic indicates the SV40 NLS. (**B**) Minimal fragment of SRSF9 required to interact with full-length ADAR2 by co-immunoprecipitation. Five different SRSF9 truncation variants (S1–S5) were tested. The short red bar in the schematic indicates the SV40 NLS. (**C**) Minimal fragment of SRSF9 protein that could repress ADAR2-mediated editing of endogenous XKR6 transcripts. Notably, NLS-RRM2 of SRSF9 (construct S5) could repress editing to the same extent as the full-length splicing factor. Error bars indicate the s.e.m. ($n = 3$ biological replicates). (**$P < 0.05$, ***$P < 0.01$; Student's t-test. There must be at least 5% change in editing levels to be considered significant). (**D**) Immunoblot showing the results of co-immunoprecipitation experiments performed without and with RNase treatment. We found that addition of RNase dramatically reduced the amount of SRSF9 protein that was pulled down with ADAR2. (**E**) Immunoblot showing the results of co-immunoprecipitation experiments to evaluate the effect of two mutations, K128A and D129A, on SRSF9's ability to interact with ADAR2. (**F**) Evaluating the ability of different SRSF9 mutant proteins to repress the editing of XKR6. Error bars indicate the s.e.m. ($n = 3$ biological replicates). (***$P < 0.01$; Student's t-test. There must be at least 5% change in editing levels to be considered significant). (**G**) Exemplary immunoblot showing the effect of SRSF9 on ADAR2 dimerization. The protein mixture was resolved by native PAGE. (**H**) Quantification of the amount of ADAR2 monomers and ADAR2 dimers without (−) or with (+) SRSF9 overexpression. Error bars indicate the s.e.m. ($n = 7$ biological replicates). Immunoblots of all the replicates are provided in Supplementary Figure S13. (***$P < 0.01$; Student's t-test).

to construct minigenes to understand the intrinsic features of transcripts whose editing could be repressed by SRSF9. We first identified the editing site complementary sequences (ECSes) of various ADAR2 substrates. For CACNA1D, we searched the flanking introns of exon 41, which contained two protein-coding sites, for highly conserved regions (Supplementary Figure S14) and found a short intronic sequence about 3800 bp upstream of the editing sites that may potentially base pair with the exon to form a dsRNA structure necessary for editing to occur. For KCNA1, SON and XKR6, the putative ECSes were relatively easier to locate as they appeared to be within the same protein-coding exons as the respective editing sites. We then used the RNAfold program from the Vienna package (52) to predict RNA struc-

tures and confirmed the stem structures for all four substrates (Supplementary Figure S15).

Since we did not know where in the transcripts SRSF9 might be binding, we started off by cloning fragments that were sizably larger than the minimal dsRNA stems necessary for editing to occur (Figure 4A). Subsequently, we introduced these minigenes into HEK293T cells to test whether they could be edited by ADAR2 and then repressed by SRSF9 (Figure 4B and Supplementary Figure S16). When the minigenes were co-transfected with an ADAR2 overexpression plasmid alone, they could be edited robustly at frequencies ranging from 27% to nearly 90%. Importantly, the editing levels were significantly lower ($P < 0.05$, Student's *t*-test) when the minigenes were co-transfected with both an ADAR2 overexpression plasmid and a SRSF9 overexpression plasmid. We further verified that similar repression of editing by SRSF9 could be observed regardless of whether we sequenced our PCR products with a forward primer or a reverse primer (Supplementary Figure S17).

Next, we explored whether it was possible to reduce the size of the KCNA1 minigene by progressively reducing the length of the original construct and also by cloning a different part of the exon containing the editing sites and the ECS (Figure 4C). We found that SRSF9 failed to repress the editing of all the smaller minigenes (Figure 4D and Supplementary Figure S18). Notably, a small fragment containing just the minimal stem structure (Variant 2) was edited robustly by ADAR2, but this editing could not be repressed by SRSF9. Hence, our results indicate that SRSF9 can regulate editing at a long distance perhaps through folding of the RNA in three-dimensional space.

A previous study showed that SRSF9 bound directly to an intronic RNA sequence CUGGAUU to regulate the splicing of hnRNP A1 pre-mRNA (35). We wondered whether SRSF9 also relied on the same sequence motif to regulate RNA editing. To this end, we examined the CACNA1D minigene and found a similar motif 20-bp downstream of the ECS (Supplementary Figure S19A), which is still within a highly conserved region of intron 40 (Supplementary Figure S14). In rodents, the genomic sequence is exactly CTGGATT, while in primates, the genomic sequence is CTGTATT and contains a single nucleotide change. To assess the functionality of the putative motif, we deleted it from the CACNA1D minigene, but found that ADAR2-mediated editing of the minigene could still be repressed by SRSF9 to a similar extent as the original minigene (Supplementary Figure S19B). Hence, it is possible that SRSF9 relies on different *cis*-acting elements to perform its two separate functions in RNA splicing and RNA editing.

Genome-wide analysis of SRSF9 binding and repression

We sought to obtain a more comprehensive global view of the SRSF9 editing regulon beyond the limited number of protein-coding sites that we had examined so far. First, we performed RNA-seq analysis to quantify changes in editing levels upon overexpression of ADAR2 alone or upon overexpression of both ADAR2 and SRSF9 (Figure 5A). We focused on the extensive list of sites in the RADAR database (53) and required a minimum coverage of 20 reads to be confident of our editing level measurements. Upon overexpression of ADAR2, we found that 18 174 sites were differentially edited compared to control cells, of which 97.0% showed a significant increase in their editing levels as expected ($P < 0.05$, Fisher's test) (Figure 5B). Furthermore, when we overexpressed both ADAR2 and SRSF9 together, we found that 6,994 sites were differentially edited compared to overexpression of the deaminase alone ($P < 0.05$, Fisher's test). Importantly, the editing of 92.5% of these sites was downregulated, consistent with the function of SRSF9 as a repressor of editing (Figure 5B). Additionally, most of the significant sites were in 3′UTR and introns, thereby extending the regulatory role of SRSF9 beyond the protein-coding region.

Subsequently, we sought to identify the editing sites that were regulated directly by SRSF9. To this end, we mapped the RNA binding sites of SRSF9 in HEK293T cells by eCLIP-seq (enhanced crosslinking followed by immunoprecipitation and deep sequencing) (42) and developed an in-house computational pipeline to analyze our deep sequencing datasets (Supplementary Figure S20). A potential confounding factor is that many of the binding sites will be irrelevant to RNA editing because SRSF9 also performs an important function in splicing. To overcome this problem, we examined the binding sites without and with overexpression of ADAR2 and then searched for sites that exhibited enhanced binding by SRSF9 in the presence of the editing enzyme (Figure 5C). Additionally, we co-transfected the original 4012-bp long CACNA1D minigene, as low expression of the endogenous gene in HEK293T cells may not allow us to determine the binding locations of SRSF9 in the CACNA1D transcripts.

Overall, our eCLIP-seq experiments yielded a total number of 80 514 binding peaks throughout the transcriptome, of which 31 772 peaks exhibited enhanced binding by SRSF9 with ADAR2 overexpression. Importantly, SRSF9 did not bind to the CACNA1D minigene when there was a lack of ADAR2 protein, but bound strongly to the minigene at two separate locations upon ADAR2 overexpression (Supplementary Figure S21A). Similarly, SRSF9 did not bind to the endogenous SON transcripts surrounding the editing sites without exogenously supplied ADAR2, but exhibited strong binding at multiple positions of the gene upon ADAR2 overexpression (Figure 5D). These two examples indicate the validity of our approach. We then shortlisted 2646 SRSF9-bound genes that also contained at least one editing site covered by a minimum of 20 reads in our RNA-seq data. Upon overlapping with the list of genes whose editing was significantly inhibited by SRSF9 based on our earlier RNA-seq analysis, we obtained a final set of 3823 sites in 683 genes (Figure 5E and Supplementary Figure S21B), which constituted the direct editing regulon of SRSF9 as supported by evidence from binding data (eCLIP-seq) and functional data (RNA-seq).

The protein-coding sites of SON lie within the direct editing regulon of SRSF9. Hence, we decided to examine the binding peaks within SON in detail. We focused on the 1 kb region surrounding the editing sites that we had earlier found to be sufficient for editing repression by SRSF9 (Figure 4A and B). There were four significant eCLIP-seq peaks in this region (Figure 5D and F). To assess their func-

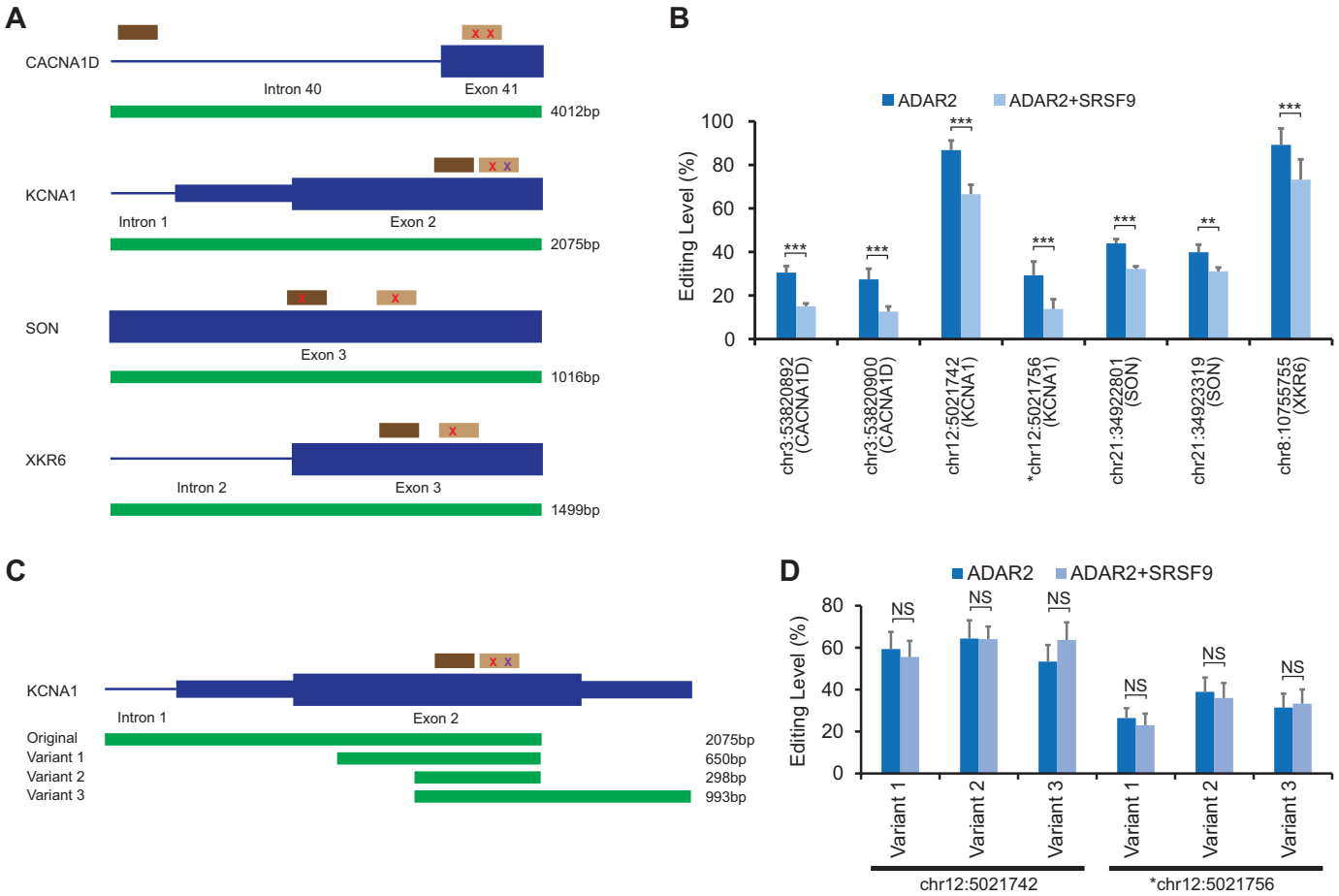

Figure 4. Analysis of minigenes. (**A**) Schematic showing four different genomic loci-of-interest. Red crosses indicate known editing sites, while the purple cross in KCNA1 indicates the novel editing site identified in this study. The light brown and dark brown bars represent the editing stem structure, while the green horizontal bars indicate our cloned minigenes. (**B**) Effect of SRSF9 on the editing of our minigenes in HEK293T cells. Error bars indicate the s.e.m. ($n \geq 3$ biological replicates). (**$P < 0.05$, ***$P < 0.01$; Student's *t*-test. All significant sites must show at least 5% change in their editing levels). (**C**) Schematic showing the KCNA1 genomic locus and the three truncated minigenes (Variant 1, Variant 2 and Variant 3) in relation to the original full-length (2075 bp) construct. (**D**) Effect of SRSF9 on the editing of the three truncated KCNA1 minigenes in HEK293T cells. Error bars indicate the s.e.m. ($n \geq 3$ biological replicates). (NS: not significant; Student's *t*-test).

tionality, we generated two variants of the SON minigene, one lacking the rightmost SRSF9 binding site (Variant 1) and another missing the binding sites at both ends (Variant 2). We found that Variant 1 could be edited and repressed just as efficiently as the original minigene for the two editing sites-of-interest (Figure 5G and Supplementary Figure S21C), thereby indicating that the rightmost binding location of SRSF9 was either non-functional or redundant. Interestingly however, while the editing and repression of the downstream site (chr21:34923319) in Variant 2 was comparable to the original minigene, we found that SRSF9 could not repress the editing of the upstream site (chr21:34922801) to the same extent as before (Figure 5G and Supplementary Figure S21C). Hence, the leftmost binding location of SRSF9 was necessary for the splicing factor to regulate the editing of the upstream but not the downstream site. The results also highlighted the usefulness of our eCLIP-seq data in identifying functional *cis*-acting elements.

Interestingly, we noted that there were 1963 genes that were bound by SRSF9 in the presence of ADAR2 but yet contained editing sites that were not repressed by the splicing factor. To rule out the possibility that the genes were simply lowly edited even with the overexpression of ADAR2, we determined the maximum editing level observed in each gene (Figure 5E). While the majority of the genes were indeed lowly edited, there were still 860 genes that were edited at a frequency of at least 5%. In fact, 425 of them were edited at a frequency of 20% or more. Hence, our data indicate that recruitment of SRSF9 to RNA substrates by ADAR2 may not necessarily result in productive repression of A-to-I editing. This might be because there can be other unknown regulatory factors present as well and the final editing level is the outcome of complex combinatorial control by multiple regulators. Nevertheless, we cannot rule out the possibility that some of the ADAR2-dependent, SRSF9-bound genes may also be non-biological targets due to SRSF9 overexpression.

We wondered whether the ability of SRSF9 to inhibit editing of a particular site could be affected by the site's distance from the bound location of SRSF9 on the transcript. To this end, we calculated the distance of each edit-

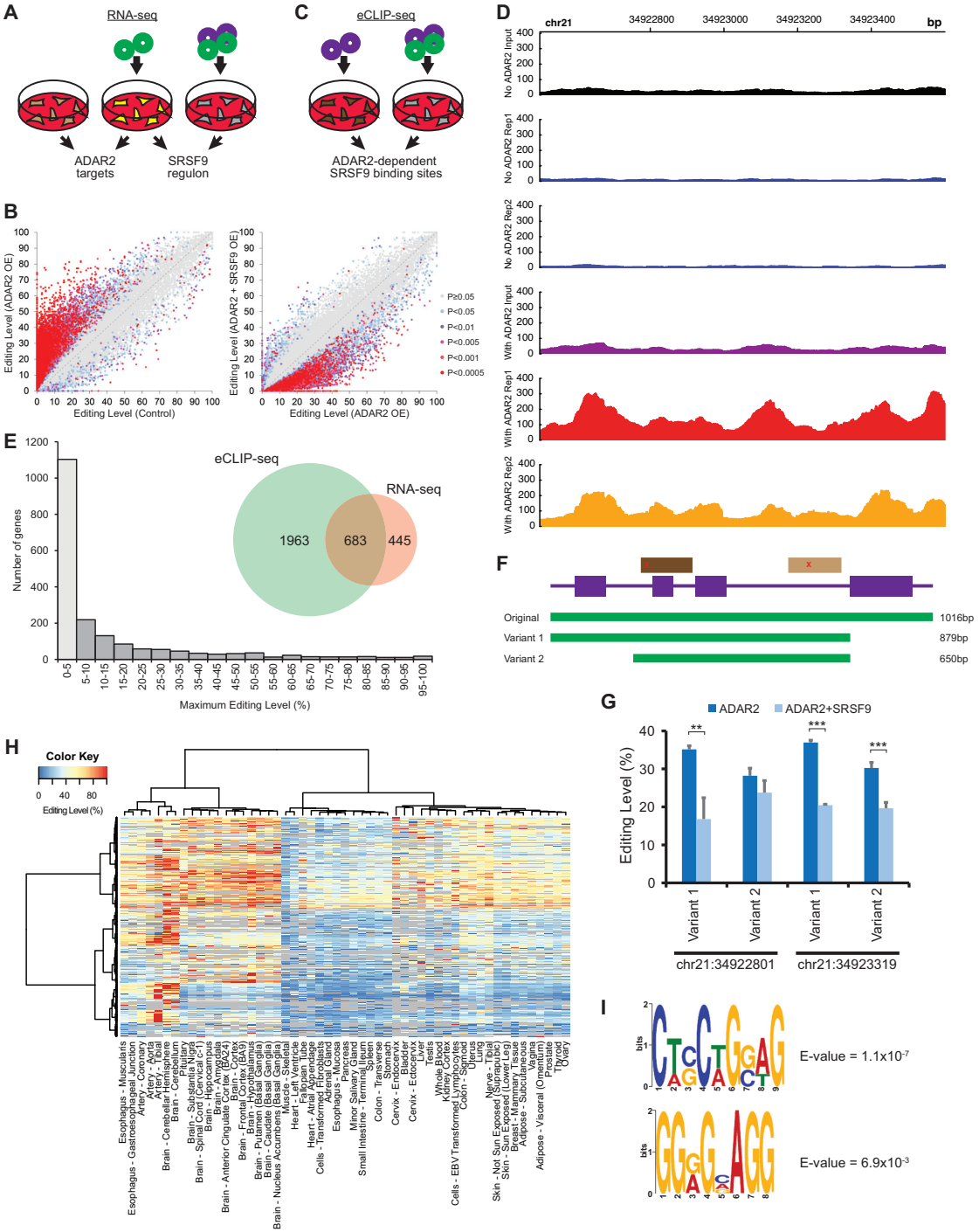

Figure 5. Genome-wide analysis of RNA editing sites regulated by SRSF9. (**A**) Schematic of experimental setup to study the regulation of editing by SRSF9 using RNA-seq. Purple rings represent plasmids encoding SRSF9, while green rings represent plasmids encoding ADAR2. (**B**) Left panel: comparison of editing levels between control cells and cells with ADAR2 overexpressed (OE). Right panel: comparison of editing levels between cells with ADAR2 overexpressed and cells with both ADAR2 and SRSF9 overexpressed. (**C**) Schematic of experimental setup to study the transcriptome-wide binding of SRSF9 using eCLIP-seq. Purple rings represent plasmids encoding SRSF9, while green rings represent plasmids encoding ADAR2. (**D**) Transcript map of SON generated from eCLIP-seq. Shown are two biological replicates for SRSF9 binding without ADAR2 overexpression, two biological replicates for SRSF9 binding with ADAR2 overexpression, as well as paired size-matched inputs. (**E**) Distribution of the maximum editing levels of genes that were bound but not regulated by SRSF9. ADAR2 recruited SRSF9 to the RNA transcripts of these genes, but the splicing factor failed to inhibit their editing. Inset: Venn diagram showing the overlap of our eCLIP-seq results and our RNA-seq results. The 683 genes in the intersection constitute the direct editing regulon of SRSF9. (**F**) Schematic showing the different SON minigenes (in green) tested. The purple boxes represent the SRSF9 binding locations in the SON transcript. The light brown and dark brown bars represent the editing stem structure, while the red crosses indicate the editing sites. (**G**) Effect of SRSF9 on the editing of the two truncated SON minigenes in HEK293T cells. Error bars indicate the s.e.m. ($n \geq 3$ biological replicates). (**$P < 0.05$, ***$P < 0.01$; Student's *t*-test. All significant sites must show at least 5% change in their editing levels). (**H**) Heatmap showing the GTEx tissue editing profiles of brain-specific sites regulated directly by SRSF9. (**I**) Enriched sequence motifs present in the ADAR2-dependent SRSF9 binding peaks.

ing site to the closest SRSF9 binding peak for both the significant set of 3823 sites in the SRSF9 regulon and the set of remaining 50 326 sites that resided in genes bound by SRSF9 but were not regulated by the splicing factor. Since the lengths of different transcripts were highly variable, we normalized the distance to gene length and plotted its distribution for both the significant set and the negative control (Supplementary Figure S21D). Overall, both distributions looked similar and we found that SRSF9 did not bind nearer to sites whose editing could be repressed by it ($P > 0.1$, Kolmogorov–Smirnov test). Hence, our genome-wide analysis suggests that SRSF9 can inhibit editing at a distance and agrees with our earlier results on the KCNA1 minigenes (Figure 4).

To gain further insights into the editing sites that were directly regulated by SRSF9, we examined their editing profiles across multiple human tissues. For this purpose, we made use of the GTEx project data on 53 distinct body sites (13 brain and 40 non-brain tissues) from 552 donors (19). We obtained 3173 editing sites from our original set of 3823 sites, after we required each site to have frequency measurements in at least one brain tissue and one non-brain tissue. Strikingly, we found that 41.9% (1328 out of 3173 sites) were edited at significantly higher levels in the brain than in non-brain tissues ($P < 0.05$, Wilcoxon test), which represented a highly significant enrichment for brain-specific editing compared to various negative controls (see 'Materials and Methods' section) ($P < 1 \times 10^{-22}$, Fisher's test) (Figure 5H and Supplementary File S1). Furthermore, Gene Ontology (GO) analysis revealed that there was an enrichment for genes involved in neurological diseases, such as cerebellar ataxia ($P < 0.001$, hypergeometric test). Additionally, we found that the ADAR2-mediated SRSF9 binding sites were significantly enriched for two sequence motifs (Figure 5I). Notably, the palindromic C-WS-C-W-G-SW-G motif is novel and is present in the leftmost binding peak that we have earlier determined to be necessary for SRSF9 to repress an editing site in SON (Figure 5G). In contrast, a search of the ADAR2-independent eCLIP-seq peaks recovered only GA-rich motifs, which is consistent with previous studies on SRSF9 and other SR proteins (Supplementary Figure S21E) (49,54). Collectively, our results suggest that SRSF9 regulates editing in a distinct manner from splicing and also underscore its importance as a repressor of brain-specific editing sites.

Physiological consequence of editing repression by SRSF9

We wondered why there was a need for SRSF9 to repress ADAR2-mediated editing in non-brain tissues. To study this question, we utilized the human neuroblastoma cell line SH-SY5Y as a model system. Several protein-coding sites in CACNA1D, CYFIP2, XKR6, and TMEM63B were not edited in SH-SY5Y (Supplementary Figure S22A–D) due to low expression of ADAR2 and high expression of SRSF9, as assayed by qRT-PCR (Supplementary Figure S22E). We first overexpressed ADAR2 to increase the editing activity in the cells and observed some reduced cell growth (Figure 6A and B), consistent with the role of ADAR2 as a tumor suppressor in several cancer types (55–57). Strikingly, when we attempted to enhance the editing activity even further by simultaneously knocking down SRSF9, we observed that the cells grew much more slowly. This retarded growth was not simply due to loss of SRSF9 because when we knocked down the splicing factor by itself, the cells proliferated at a rate similar to the cells with ADAR2 overexpressed alone. We also measured cell viability of the different cell lines using PrestoBlue and obtained results that mirrored the growth curves (Figure 6C). Notably, when we overexpressed a catalytically dead ADAR2 enzyme (dADAR2) in our SRSF9 knockdown cells, the proliferation rate and cell viability were only marginally reduced, suggesting that the editing activity of ADAR2 was required for the observed phenotypes (Supplementary Figure S22F and G). To further confirm our results, we treated control and genetically perturbed cells with 1 μM staurosporine for 1 h and then quantified the percentage of apoptotic cells by Annexin V staining and flow cytometry (Figure 6D). We found that 3.9% of ADAR2 overexpressed cells and 5.1% of SRSF9 depleted cells were apoptotic. In contrast, 25.8% of cells with both ADAR2 overexpressed and SRSF9 depleted but only 1.4% of control cells were apoptotic.

To gain insights into the molecular underpinnings of the reduced growth rate and cell viability, we performed RNA-seq analysis of our control and genetically perturbed SH-SY5Y cells. Principal component analysis (PCA) of gene expression levels showed that the samples segregated by experimental conditions, with the first two principal components accounting for ∼70% of the variation in transcript levels (Figure 7A). Hierarchical clustering also revealed distinct patterns of gene expression between the four experimental conditions (Figure 7B). Of particular interest were the set of genes that were differentially expressed between the ADAR2-overexpressed, SRSF9-depleted cells and the more viable cells with only a single gene perturbation (Supplementary File S2). GO analysis of the upregulated genes revealed that they were enriched for functions in RNA splicing, oxidative phosphorylation, ribosome and translation-related processes, proteasome, steroid biosynthesis and RNA polymerase (Figure 7C). On the other hand, GO analysis of the downregulated genes recovered terms that were primarily related to stress responses (Figure 7D). For example, selenoamino acids, namely selenocysteine and selenomethionine, are incorporated in proteins that are involved in antioxidant activity. This may explain why the ADAR2-overexpressed, SRSF9-depleted cells were more susceptible to apoptosis, as their cellular defense mechanisms have been switched off or toned down.

Next, we quantified changes in editing levels using the RNA-seq data (Figure 7E). As before, we required a minimum coverage of 20 reads and focused on the extensive list of sites in the RADAR database (53). Expectedly, 25 508 sites were differentially edited upon ADAR2 overexpression vis-à-vis control cells, of which 97.4% showed a significant increase in their editing levels ($P < 0.05$, Fisher's test). Additionally, consistent with the role of SRSF9 as a repressor of editing, 86.7% of the 3534 differentially edited sites showed significantly increased editing levels upon SRSF9 knockdown compared to control cells ($P < 0.05$, Fisher's test). We further found that when we simultaneously overexpressed ADAR2 and depleted SRSF9, 14 640 sites were

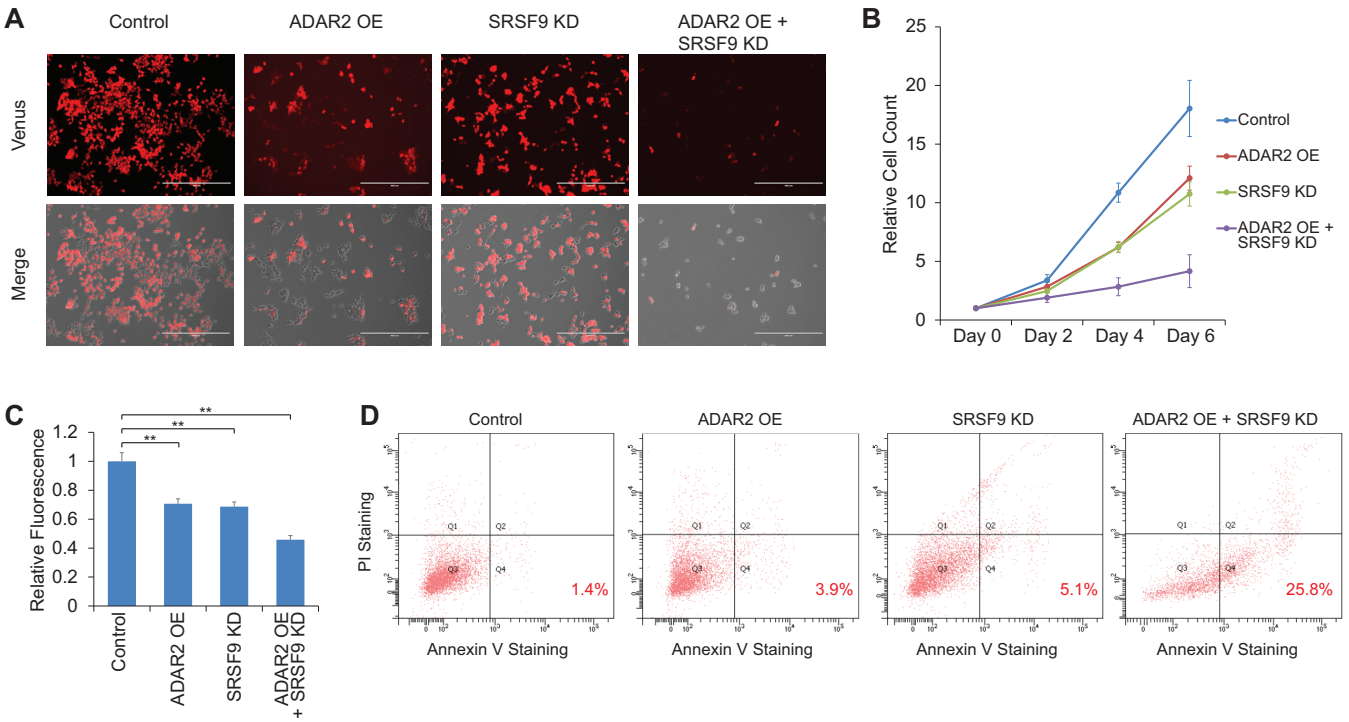

Figure 6. Effect of ADAR2 overexpression and SRSF9 knockdown on cellular behavior. (**A**) Microscopy images of different groups of cells taken 48 h after seeding at a density of 200 000 cells per well. Our plasmids carried a Venus expression cassette. (**B**) SH-SY5Y growth curves over 6 days of culture for the different groups of cells. (**C**) Results of cell viability assay using PrestoBlue. Error bars indicate the s.e.m. ($n \geq 2$ biological replicates). (**$P < 0.05$; Student's *t*-test). (**D**) SH-SY5Y cells were stained with Alexa Fluor 647 Annexin V and propidium iodide (PI) and analyzed by flow cytometry. In each panel, the lower right quadrant shows cells that are in the early stage of apoptosis, while the upper right quadrant shows cells that are in the late stage of apoptosis.

differentially edited relative to control cells, of which 95.5% exhibited significantly increased editing levels ($P < 0.05$, Fisher's test). Oddly, while the editing activity in these cells was clearly stronger than that in control cells and also in SRSF9 depleted cells, it appeared to be weaker than the editing activity in cells with ADAR2 overexpressed alone. We then checked the transcript and protein levels of ADAR2 together with a β-actin control. While there was no abnormality in the transcript levels (Supplementary Figure S23A), we were surprised to discover that we could not detect any β-actin protein in the ADAR2-overexpressed, SRSF9-depleted cells and that the ADAR2 protein level itself was not higher than that in both the control cells and the SRSF9 knockdown cells (Supplementary Figure S23B). Hence, there appeared to be a massive remodeling of the cellular proteome, given that our gene expression analysis had earlier uncovered many genes related to the proteasome and ubiquitin-linked proteolysis that were significantly upregulated upon simultaneous perturbations of ADAR2 and SRSF9 (Figure 7C).

Subsequently, we examined the 2762 sites whose editing was significantly increased in the ADAR2 overexpression plus SRSF9 knockdown condition, but not in either of the single gene perturbation condition ($P < 0.05$, Fisher's test) (Figure 7F and Supplementary File S3). GO analysis uncovered terms related to the cell cycle and mitosis as well as terms related to cellular structures that undergo dynamic changes in cell division, such as the cytoskeleton and the chromosomes, thereby suggesting that RNA editing may be involved in the dramatic reduction in cell growth. Genes with functions in DNA damage and DNA repair were also enriched, suggesting a link between editing and the cells' susceptibility to apoptosis when stressed. Notably, we further observed that the 2762 dysregulated editing sites were enriched in genes with functions related to the ribosome, mitochondrion and spliceosome, which we had earlier found to be affected when we performed GO analysis on the differentially expressed genes (Figure 7C). Importantly, the changes in editing levels were not simply due to changes in expression levels, as the set of differentially expressed genes was distinct from the set of differentially edited genes whose transcript levels remained nearly stable (Supplementary Figure S24). Hence, the functional convergence on common biological processes despite the distinct gene sets implicates RNA editing in the observed phenotypes. Collectively, our results suggest that SRSF9 prevents loss of cell viability by blocking ADAR2-mediated editing of key sites in genes that perform important functions in protein and energy metabolism as well as the cell cycle.

DISCUSSION

A-to-I RNA editing, catalyzed by the ADAR family of enzymes, is a fundamental post-transcriptional modification in animals. It has to be carefully regulated given its critical importance in many cellular processes. In a recent effort to build a comprehensive reference atlas for the scientific

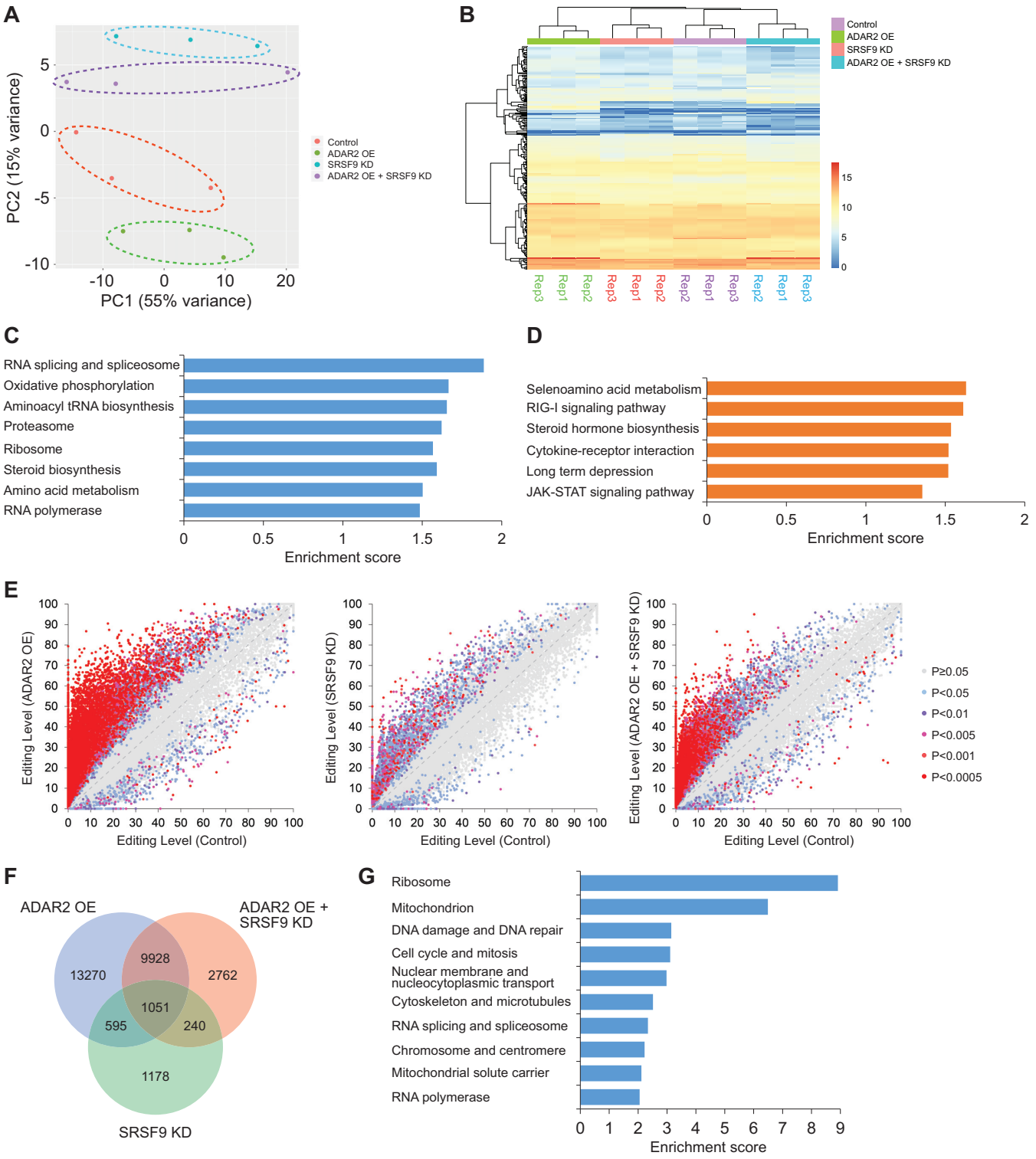

Figure 7. Transcriptome analysis of genetically perturbed SH-SY5Y cells. (**A**) PCA of gene expression levels. Three biological replicates were generated for each experimental condition. Lowly expressed genes (DESeq2 count < 10) and genes with little variation in expression across all samples (coefficient of variation < 0.1) were discarded. (**B**) Hierarchical clustering of our gene expression data. The heatmap showed that the various samples grouped according to experiment conditions. (Rep: replicate number). (**C**) GO analysis of the genes whose expression was significantly upregulated in the ADAR2-overexpressed, SRSF9-depleted cells. All the functional terms with an enrichment score of at least one (approximately $P < 0.1$) are listed. (**D**) GO analysis of the genes whose expression was significantly downregulated in the ADAR2-overexpressed, SRSF9-depleted cells. All the functional terms with an enrichment score of at least one are listed. (**E**) Left panel: comparison of editing levels between control cells and cells with ADAR2 overexpressed (OE). Middle panel: Comparison of editing levels between control cells and cells with SRSF9 knocked down (KD). Right panel: comparison of editing levels between control cells and cells with both ADAR2 OE and SRSF9 KD. (**F**) Venn diagram comparing the sites whose editing levels exhibited a significant increase in each of the three different genetic perturbation conditions. (**G**) GO analysis of the 2762 editing sites that were significantly upregulated in the ADAR2-overexpressed, SRSF9-depleted cells but not in the ADAR2-overexpressed cells or the SRSF9-depleted cells. The top 10 functional terms are listed.

community, we uncovered diverse spatiotemporal patterns of RNA editing in human (19). An open question that arises is how these patterns can be generated with only two catalytically active enzymes, ADAR1 and ADAR2. In particular, many editing sites are more highly edited in the brain than in non-brain tissues. Such a pattern can be readily accounted for in the mouse simply by the higher expression of the editing enzymes in the brain. However, the same is not true in human because ADAR1 and ADAR2 are also highly expressed in several non-brain tissues, such as the lung.

Here, we report that the splicing factor SRSF9 selectively represses the editing of numerous sites in non-brain tissues, thereby allowing them to be more highly edited in the brain. Mechanistically, we found that the RRM2 domain of SRSF9 alone is sufficient to biochemically interact with ADAR2 in the nucleus to repress editing. The dispensability of the RRM1 domain of SRSF9 for interaction and editing repression is consistent with previous work that demonstrates that a related protein SRSF1 uses only its pseudo-RRM domain (RRM2) to recognize its natural substrates in the cell (49).

In contrast to an earlier study (40), we found that the RNA substrate plays an important role in mediating SRSF9′s regulatory function in editing. RNase treatment or mutations in an RNA-binding α-helix located within RRM2 (49) abolished the interaction between SRSF9 and ADAR2 and prevented the splicing factor from inhibiting editing. The discrepancy between our work and the previous study may be due to different concentrations of RNase used or different durations of RNase treatment. Additionally, our data indicate that SRSF9 may not necessarily bind close to target sites to repress editing. It may be possible that looping of the RNA in three-dimensional space brings the splicing factor nearer to editing sites for it to perform its function, which will again require the RNA to play a more prominent role in the process.

Our experiments indicate that SRSF9 potentially interferes with the formation of ADAR2 dimers. The requirement for protein dimerization in RNA editing has been previously suggested by multiple studies (50,51,58–61), with a subset of these pinpointing dsRBD1 as the key domain involved in the process. In addition, a solution structure of the two dsRNA-binding domains of ADAR2 bound to a stem-loop pre-mRNA substrate showed that they occupy only one-third of the space around the RNA helix, indicating that the binding of a second ADAR2 molecule would be sterically possible (62). Our biochemical data are consistent with all these previous studies. However, it is currently unclear how exactly SRSF9 affects the level of ADAR2 dimers in the cell. For example, the splicing factor may bind to an ADAR2 monomer–RNA complex and prevent the recruitment of an additional ADAR2 molecule or it may bind to an already formed ADAR2 homodimer sitting on a transcript and disrupt this dimer. More work is needed to dissect the detailed mechanism underlying editing repression by SRSF9.

A natural question that arises is how SRSF9 selects particular RNA substrates for editing repression. We searched the ADAR2-dependent SRSF9 binding sites for potential sequence signatures and discovered a novel palindromic motif, C-WS-C-W-G-SW-G, that can help explain some of the brain-specific editing that we have observed, for example in the SON gene. In contrast, we were only able to recover GA-rich motifs when we searched the ADAR2-independent SRSF9 binding peaks, which is in agreement with previous studies on SRSF9 and other SR proteins (49,54). Despite this discovery, however, there are still many genes whose editing is brain-specific and is repressed by the splicing factor but yet their SRSF9 binding sites do not contain the novel palindromic motif or a GA-rich motif. One possibility is that SRSF9 might also rely on a higher-order structural motif to perform its regulatory function. Future directions could include utilizing novel techniques like PARIS (63), SPLASH (64) or LIGR-seq (65) to map RNA–RNA interactions *in vivo* and to gain structural information on the editing substrates in their native cellular context.

We have explored the question of why the editing of brain-specific sites needs to be repressed in non-brain tissues. Concomitant ADAR2 overexpression and SRSF9 depletion in the SH-SY5Y cell line resulted in a severe reduction in growth rate and cell viability, which was not observed when we perturbed the expression of ADAR2 or SRSF9 alone. The ADAR2-overexpressed, SRSF9-depleted cells were also highly susceptible to apoptosis when stressed. RNA-seq analysis revealed that the expression of genes involved in different pathways necessary for cells to cope with stresses were strongly downregulated. Importantly, GO analysis of differentially expressed genes and GO analysis of differentially edited genes converged on similar functional terms related to protein homeostasis (proteostasis) and energy metabolism. The differentially edited genes were also enriched for functions related to the cell cycle as well as DNA damage and repair. Hence, although the poor growth and cell viability of ADAR2-overexpressed, SRSF9-depleted cells may simply be an outcome compounded by two separate stressors, RNA editing is likely to play an important role due to its association with multiple dysregulated biological processes. Nevertheless, further work is needed to carefully dissect the underlying mechanism linking editing with the observed phenotypes.

In the current work, we have focused mainly on addressing brain-specific editing, but there are many other spatiotemporal editing patterns (19). For example, thousands of sites are selectively edited in only a single tissue, such as the artery. Also, we have found that an editing site's dependence on ADAR1 or ADAR2 can change depending on the biological context. Clearly, there must be other *trans*-acting factors that regulate the activity of the two deaminases.

Since we have shown that SRSF9 plays an important role in shaping the editing landscape in mammals, it is tempting to speculate that other spliceosome components may also regulate editing. Indeed, a previous study reported that ADAR2 was associated with various splicing factors, including SR proteins, in large nuclear ribonucleoprotein (lnRNP) particles (66). Additionally, the pre-mRNA undergoes many RNA processing steps before emerging from the nucleus as a mature mRNA. Hence, many RNA-binding proteins must assemble on the RNA transcript at different stages of the maturation process. It will be interesting to unravel the timing and coordination of the various events occurring on the pre-mRNA and how the different RNA processing steps influence one another.

DATA AVAILABILITY

All of the RNA-seq and eCLIP-seq data for this paper have been submitted to the NCBI Gene Expression Omnibus (GEO) (http://www.ncbi.nlm.nih.gov/geo/) under accession number GSE108127.

SUPPLEMENTARY DATA

Supplementary Data are available at NAR Online.

ACKNOWLEDGEMENTS

We thank Gene W Yeo, Eric L Van Nostrand and Gabriel A Pratt for help with the bioinformatics analysis of our eCLIP datasets. We also thank Yue Wan and the Tan lab for discussions and critical reading of the manuscript.
Authors' contribution: M.H.T. conceived the project and provided overall supervision. R.S. and M.H.T. designed the experiments. R.S., C.R.J.L., K.I.L., C.W.A.W., Z.H.M.C. and M.H.T. performed the experiments. F.Z., H.S., X.Z. and M.H.T. analyzed the Illumina sequencing data. J.P.B. and M.M. provided the monkey tissues. R.S. and M.H.T. wrote the manuscript with inputs from the other authors.

FUNDING

Nanyang Technological University School of Chemical and Biomedical Engineering (to M.H.T.); Genome Institute of Singapore (to M.H.T.); National Medical Research Council OFIRG15nov151 (to M.H.T.); National Medical Research Council CBRG14may003 (to M.H.T.). Funding for open access charge: Genome Institute of Singapore.
Conflict of interest statement. None declared.

REFERENCES

1. Nishikura,K. (2010) Functions and regulation of RNA editing by ADAR deaminases. *Annu. Rev. Biochem.*, **79**, 321–349.
2. Bahn,J.H., Lee,J.H., Li,G., Greer,C., Peng,G. and Xiao,X. (2012) Accurate identification of A-to-I RNA editing in human by transcriptome sequencing. *Genome Res.*, **22**, 142–150.
3. Danecek,P., Nellaker,C., McIntyre,R.E., Buendia-Buendia,J.E., Bumpstead,S., Ponting,C.P., Flint,J., Durbin,R., Keane,T.M. and Adams,D.J. (2012) High levels of RNA-editing site conservation amongst 15 laboratory mouse strains. *Genome Biol.*, **13**, 26.
4. Li,J.B., Levanon,E.Y., Yoon,J.K., Aach,J., Xie,B., Leproust,E., Zhang,K., Gao,Y. and Church,G.M. (2009) Genome-wide identification of human RNA editing sites by parallel DNA capturing and sequencing. *Science*, **324**, 1210–1213.
5. Peng,Z., Cheng,Y., Tan,B.C., Kang,L., Tian,Z., Zhu,Y., Zhang,W., Liang,Y., Hu,X., Tan,X. *et al.* (2012) Comprehensive analysis of RNA-Seq data reveals extensive RNA editing in a human transcriptome. *Nat. Biotechnol.*, **30**, 253–260.
6. Ramaswami,G., Lin,W., Piskol,R., Tan,M.H., Davis,C. and Li,J.B. (2012) Accurate identification of human Alu and non-Alu RNA editing sites. *Nat. Methods*, **9**, 579–581.
7. Ramaswami,G., Zhang,R., Piskol,R., Keegan,L.P., Deng,P., O'Connell,M.A. and Li,J.B. (2013) Identifying RNA editing sites using RNA sequencing data alone. *Nat. Methods*, **10**, 128–132.
8. St Laurent,G., Tackett,M.R., Nechkin,S., Shtokalo,D., Antonets,D., Savva,Y.A., Maloney,R., Kapranov,P., Lawrence,C.E. and Reenan,R.A. (2013) Genome-wide analysis of A-to-I RNA editing by single-molecule sequencing in Drosophila. *Nat. Struct. Mol. Biol.*, **20**, 1333–1339.
9. Washburn,M.C., Kakaradov,B., Sundararaman,B., Wheeler,E., Hoon,S., Yeo,G.W. and Hundley,H.A. (2014) The dsRBP and inactive editor ADR-1 utilizes dsRNA binding to regulate A-to-I RNA editing across the C. elegans transcriptome. *Cell Rep.*, **6**, 599–607.
10. Zhao,H.Q., Zhang,P., Gao,H., He,X., Dou,Y., Huang,A.Y., Liu,X.M., Ye,A.Y., Dong,M.Q. and Wei,L. (2015) Profiling the RNA editomes of wild-type C. elegans and ADAR mutants. *Genome Res.*, **25**, 66–75.
11. Goldstein,B., Agranat-Tamir,L., Light,D., Ben-Naim Zgayer,O., Fishman,A. and Lamm,A.T. (2017) A-to-I RNA editing promotes developmental stage-specific gene and lncRNA expression. *Genome Res.*, **27**, 462–470.
12. Chen,L., Li,Y., Lin,C.H., Chan,T.H., Chow,R.K., Song,Y., Liu,M., Yuan,Y.F., Fu,L., Kong,K.L. *et al.* (2013) Recoding RNA editing of AZIN1 predisposes to hepatocellular carcinoma. *Nat. Med.*, **19**, 209–216.
13. Qin,Y.R., Qiao,J.J., Chan,T.H., Zhu,Y.H., Li,F.F., Liu,H., Fei,J., Li,Y., Guan,X.Y. and Chen,L. (2014) Adenosine-to-inosine RNA editing mediated by ADARs in esophageal squamous cell carcinoma. *Cancer Res.*, **74**, 840–851.
14. Chan,T.H., Qamra,A., Tan,K.T., Guo,J., Yang,H., Qi,L., Lin,J.S., Ng,V.H., Song,Y., Hong,H. *et al.* (2016) ADAR-Mediated RNA editing predicts progression and prognosis of gastric cancer. *Gastroenterology*, **151**, 637–650.
15. Kubota-Sakashita,M., Iwamoto,K., Bundo,M. and Kato,T. (2014) A role of ADAR2 and RNA editing of glutamate receptors in mood disorders and schizophrenia. *Mol. Brain*, **7**, 5.
16. Kawahara,Y., Ito,K., Sun,H., Aizawa,H., Kanazawa,I. and Kwak,S. (2004) Glutamate receptors: RNA editing and death of motor neurons. *Nature*, **427**, 801.
17. Hwang,T., Park,C.K., Leung,A.K., Gao,Y., Hyde,T.M., Kleinman,J.E., Rajpurohit,A., Tao,R., Shin,J.H. and Weinberger,D.R. (2016) Dynamic regulation of RNA editing in human brain development and disease. *Nat. Neurosci.*, **19**, 1093–1099.
18. Khermesh,K., D'Erchia,A.M., Barak,M., Annese,A., Wachtel,C., Levanon,E.Y., Picardi,E. and Eisenberg,E. (2016) Reduced levels of protein recoding by A-to-I RNA editing in Alzheimer's disease. *RNA*, **22**, 290–302.
19. Tan,M.H., Li,Q., Shanmugam,R., Piskol,R., Kohler,J., Young,A.N., Liu,K.I., Zhang,R., Ramaswami,G., Ariyoshi,K. *et al.* (2017) Dynamic landscape and regulation of RNA editing in mammals. *Nature*, **550**, 249–254.
20. Wang,Q., Khillan,J., Gadue,P. and Nishikura,K. (2000) Requirement of the RNA editing deaminase ADAR1 gene for embryonic erythropoiesis. *Science*, **290**, 1765–1768.
21. Wang,Q., Miyakoda,M., Yang,W., Khillan,J., Stachura,D.L., Weiss,M.J. and Nishikura,K. (2004) Stress-induced apoptosis associated with null mutation of ADAR1 RNA editing deaminase gene. *J. Biol. Chem.*, **279**, 4952–4961.
22. Hartner,J.C., Schmittwolf,C., Kispert,A., Muller,A.M., Higuchi,M. and Seeburg,P.H. (2004) Liver disintegration in the mouse embryo caused by deficiency in the RNA-editing enzyme ADAR1. *J. Biol. Chem.*, **279**, 4894–4902.
23. Liddicoat,B.J., Piskol,R., Chalk,A.M., Ramaswami,G., Higuchi,M., Hartner,J.C., Li,J.B., Seeburg,P.H. and Walkley,C.R. (2015) RNA editing by ADAR1 prevents MDA5 sensing of endogenous dsRNA as nonself. *Science*, **349**, 1115–1120.
24. Higuchi,M., Maas,S., Single,F.N., Hartner,J., Rozov,A., Burnashev,N., Feldmeyer,D., Sprengel,R. and Seeburg,P.H. (2000) Point mutation in an AMPA receptor gene rescues lethality in mice deficient in the RNA-editing enzyme ADAR2. *Nature*, **406**, 78–81.
25. George,C.X. and Samuel,C.E. (1999) Human RNA-specific adenosine deaminase ADAR1 transcripts possess alternative exon 1 structures that initiate from different promoters, one constitutively active and the other interferon inducible. *Proc. Natl. Acad. Sci. U.S.A.*, **96**, 4621–4626.
26. Patterson,J.B. and Samuel,C.E. (1995) Expression and regulation by interferon of a double-stranded-RNA-specific adenosine deaminase from human cells: evidence for two forms of the deaminase. *Mol. Cell. Biol.*, **15**, 5376–5388.
27. Peng,P.L., Zhong,X., Tu,W., Soundarapandian,M.M., Molner,P., Zhu,D., Lau,L., Liu,S., Liu,F. and Lu,Y. (2006) ADAR2-dependent RNA editing of AMPA receptor subunit GluR2 determines vulnerability of neurons in forebrain ischemia. *Neuron*, **49**, 719–733.

28. Lee,S., Yang,G., Yong,Y., Liu,Y., Zhao,L., Xu,J., Zhang,X., Wan,Y., Feng,C., Fan,Z. *et al.* (2010) ADAR2-dependent RNA editing of GluR2 is involved in thiamine deficiency-induced alteration of calcium dynamics. *Mol. Neurodegener.*, **5**, 54.
29. Rueter,S.M., Dawson,T.R. and Emeson,R.B. (1999) Regulation of alternative splicing by RNA editing. *Nature*, **399**, 75–80.
30. Desterro,J.M., Keegan,L.P., Jaffray,E., Hay,R.T., O'Connell,M.A. and Carmo-Fonseca,M. (2005) SUMO-1 modification alters ADAR1 editing activity. *Mol. Biol. Cell*, **16**, 5115–5126.
31. Marcucci,R., Brindle,J., Paro,S., Casadio,A., Hempel,S., Morrice,N., Bisso,A., Keegan,L.P., Del Sal,G. and O'Connell,M.A. (2011) Pin1 and WWP2 regulate GluR2 Q/R site RNA editing by ADAR2 with opposing effects. *EMBO J.*, **30**, 4211–4222.
32. Sansam,C.L., Wells,K.S. and Emeson,R.B. (2003) Modulation of RNA editing by functional nucleolar sequestration of ADAR2. *Proc. Natl. Acad. Sci. U.S.A.*, **100**, 14018–14023.
33. Desterro,J.M., Keegan,L.P., Lafarga,M., Berciano,M.T., O'Connell,M. and Carmo-Fonseca,M. (2003) Dynamic association of RNA-editing enzymes with the nucleolus. *J. Cell Sci.*, **116**, 1805–1818.
34. Bourgeois,C.F., Lejeune,F. and Stevenin,J. (2004) Broad specificity of SR (serine/arginine) proteins in the regulation of alternative splicing of pre-messenger RNA. *Prog. Nucleic Acid Res. Mol. Biol.*, **78**, 37–88.
35. Simard,M.J. and Chabot,B. (2002) SRp30c is a repressor of 3′ splice site utilization. *Mol. Cell. Biol.*, **22**, 4001–4010.
36. Wang,Y., Wang,J., Gao,L., Lafyatis,R., Stamm,S. and Andreadis,A. (2005) Tau exons 2 and 10, which are misregulated in neurodegenerative diseases, are partly regulated by silencers which bind a SRp30c.SRp55 complex that either recruits or antagonizes htra2beta1. *J. Biol. Chem.*, **280**, 14230–14239.
37. Cloutier,P., Toutant,J., Shkreta,L., Goekjian,S., Revil,T. and Chabot,B. (2008) Antagonistic effects of the SRp30c protein and cryptic 5′ splice sites on the alternative splicing of the apoptotic regulator Bcl-x. *J. Biol. Chem.*, **283**, 21315–21324.
38. Huang,Y. and Steitz,J.A. (2005) SRprises along a messenger's journey. *Mol. Cell*, **17**, 613–615.
39. Long,J.C. and Caceres,J.F. (2009) The SR protein family of splicing factors: master regulators of gene expression. *Biochem. J.*, **417**, 15–27.
40. Tariq,A., Garncarz,W., Handl,C., Balik,A., Pusch,O. and Jantsch,M.F. (2013) RNA-interacting proteins act as site-specific repressors of ADAR2-mediated RNA editing and fluctuate upon neuronal stimulation. *Nucleic Acids Res.*, **41**, 2581–2593.
41. Bratt,E. and Ohman,M. (2003) Coordination of editing and splicing of glutamate receptor pre-mRNA. *RNA*, **9**, 309–318.
42. Van Nostrand,E.L., Pratt,G.A., Shishkin,A.A., Gelboin-Burkhart,C., Fang,M.Y., Sundararaman,B., Blue,S.M., Nguyen,T.B., Surka,C., Elkins,K. *et al.* (2016) Robust transcriptome-wide discovery of RNA-binding protein binding sites with enhanced CLIP (eCLIP). *Nat. Methods*, **13**, 508–514.
43. Zhang,R., Li,X., Ramaswami,G., Smith,K.S., Turecki,G., Montgomery,S.B. and Li,J.B. (2014) Quantifying RNA allelic ratios by microfluidic multiplex PCR and sequencing. *Nat. Methods*, **11**, 51–54.
44. Burns,C.M., Chu,H., Rueter,S.M., Hutchinson,L.K., Canton,H., Sanders-Bush,E. and Emeson,R.B. (1997) Regulation of serotonin-2C receptor G-protein coupling by RNA editing. *Nature*, **387**, 303–308.
45. Sommer,B., Kohler,M., Sprengel,R. and Seeburg,P.H. (1991) RNA editing in brain controls a determinant of ion flow in glutamate-gated channels. *Cell*, **67**, 11–19.
46. Ohlson,J., Pedersen,J.S., Haussler,D. and Ohman,M. (2007) Editing modifies the GABA(A) receptor subunit alpha3. *RNA*, **13**, 698–703.
47. Bhalla,T., Rosenthal,J.J., Holmgren,M. and Reenan,R. (2004) Control of human potassium channel inactivation by editing of a small mRNA hairpin. *Nat. Struct. Mol. Biol.*, **11**, 950–956.
48. Maas,S. and Gommans,W.M. (2009) Identification of a selective nuclear import signal in adenosine deaminases acting on RNA. *Nucleic Acids Res.*, **37**, 5822–5829.
49. Clery,A., Sinha,R., Anczukow,O., Corrionero,A., Moursy,A., Daubner,G.M., Valcarcel,J., Krainer,A.R. and Allain,F.H. (2013) Isolated pseudo-RNA-recognition motifs of SR proteins can regulate splicing using a noncanonical mode of RNA recognition. *Proc. Natl. Acad. Sci. U.S.A.*, **110**, E2802–E2811.
50. Gallo,A., Keegan,L.P., Ring,G.M. and O'Connell,M.A. (2003) An ADAR that edits transcripts encoding ion channel subunits functions as a dimer. *EMBO J.*, **22**, 3421–3430.
51. Poulsen,H., Jorgensen,R., Heding,A., Nielsen,F.C., Bonven,B. and Egebjerg,J. (2006) Dimerization of ADAR2 is mediated by the double-stranded RNA binding domain. *RNA*, **12**, 1350–1360.
52. Lorenz,R., Bernhart,S.H., Honer,Z.U., Siederdissen,C., Tafer,H., Flamm,C., Stadler,P.F. and Hofacker,I.L. (2011) ViennaRNA package 2.0. *Algorithms Mol. Biol.*, **6**, 26.
53. Ramaswami,G. and Li,J.B. (2014) RADAR: a rigorously annotated database of A-to-I RNA editing. *Nucleic Acids Res.*, **42**, D109–D113.
54. Ray,D., Kazan,H., Cook,K.B., Weirauch,M.T., Najafabadi,H.S., Li,X., Gueroussov,S., Albu,M., Zheng,H., Yang,A. *et al.* (2013) A compendium of RNA-binding motifs for decoding gene regulation. *Nature*, **499**, 172–177.
55. Galeano,F., Rossetti,C., Tomaselli,S., Cifaldi,L., Lezzerini,M., Pezzullo,M., Boldrini,R., Massimi,L., Di Rocco,C.M., Locatelli,F. *et al.* (2013) ADAR2-editing activity inhibits glioblastoma growth through the modulation of the CDC14B/Skp2/p21/p27 axis. *Oncogene*, **32**, 998–1009.
56. Chan,T.H., Lin,C.H., Qi,L., Fei,J., Li,Y., Yong,K.J., Liu,M., Song,Y., Chow,R.K., Ng,V.H. *et al.* (2014) A disrupted RNA editing balance mediated by ADARs (Adenosine DeAminases that act on RNA) in human hepatocellular carcinoma. *Gut*, **63**, 832–843.
57. Chen,Y.B., Liao,X.Y., Zhang,J.B., Wang,F., Qin,H.D., Zhang,L., Shugart,Y.Y., Zeng,Y.X. and Jia,W.H. (2017) ADAR2 functions as a tumor suppressor via editing IGFBP7 in esophageal squamous cell carcinoma. *Int. J. Oncol.*, **50**, 622–630.
58. Jaikaran,D.C.J., Collins,C.H. and MacMillan,A.M. (2002) Adenosine to inosine editing by ADAR2 requires formation of a ternary complex on the GluR-B R/G site. *J. Biol. Chem.*, **277**, 37624–37629.
59. Cho,D.-S.C., Yang,W., Lee,J.T., Shiekhattar,R., Murray,J.M. and Nishikura,K. (2003) Requirement of dimerization for RNA editing activity of adenosine deaminases acting on RNA. *J. Biol. Chem.*, **278**, 17093–17102.
60. Chilibeck,K.A., Wu,T., Liang,C., Schellenberg,M.J., Gesner,E.M., Lynch,J.M. and MacMillan,A.M. (2006) FRET analysis ofin VivoDimerization by RNA-editing enzymes. *J. Biol. Chem.*, **281**, 16530–16535.
61. Valente,L. and Nishikura,K. (2007) RNA Binding-independent dimerization of adenosine deaminases acting on RNA and dominant negative effects of nonfunctional subunits on dimer functions. *J. Biol. Chem.*, **282**, 16054–16061.
62. Stefl,R., Oberstrass,F.C., Hood,J.L., Jourdan,M., Zimmermann,M., Skrisovska,L., Maris,C., Peng,L., Hofr,C., Emeson,R.B. *et al.* (2010) The solution structure of the ADAR2 dsRBM-RNA complex reveals a sequence-specific readout of the minor groove. *Cell*, **143**, 225–237.
63. Lu,Z., Zhang,Q.C., Lee,B., Flynn,R.A., Smith,M.A., Robinson,J.T., Davidovich,C., Gooding,A.R., Goodrich,K.J., Mattick,J.S. *et al.* (2016) RNA duplex map in living cells reveals Higher-Order transcriptome structure. *Cell*, **165**, 1267–1279.
64. Aw,J.G., Shen,Y., Wilm,A., Sun,M., Lim,X.N., Boon,K.L., Tapsin,S., Chan,Y.S., Tan,C.P., Sim,A.Y. *et al.* (2016) In vivo mapping of eukaryotic RNA interactomes reveals principles of Higher-Order organization and regulation. *Mol. Cell*, **62**, 603–617.
65. Sharma,E., Sterne-Weiler,T., O'Hanlon,D. and Blencowe,B.J. (2016) Global mapping of human RNA-RNA interactions. *Mol. Cell*, **62**, 618–626.
66. Raitskin,O., Cho,D.S., Sperling,J., Nishikura,K. and Sperling,R. (2001) RNA editing activity is associated with splicing factors in lnRNP particles: The nuclear pre-mRNA processing machinery. *Proc. Natl. Acad. Sci. U.S.A.*, **98**, 6571–6576.